J. Fluid Mech. (1972), *vol.* 54, *part* 3, *pp.* 521–543
Printed in Great Britain

Bounds for heat transport in a porous layer

By F. H. BUSSE

Department of Planetary and Space Sciences,
University of California, Los Angeles

AND D. D. JOSEPH

Department of Aerospace Engineering and Mechanics,
University of Minnesota

(Received 20 September 1971)

Bounds on the heat transport in a porous layer are derived using the variational method of Howard (1963) and Busse (1969*b*). The relatively simple structure of the variational problem in the case of porous convection allows one to formulate the theory more simply and to investigate some of the mathematical questions posed by the earlier work. A precise characterization of the solution with N wavenumbers is given. The variational problem is solved exactly among functions with a single overall wavenumber and this solution is in good agreement with a nonlinear perturbation solution of the governing equations and with experiments. An N-wavenumber solution is constructed for large Nusselt numbers by boundary-layer methods. The asymptotic solution is compared with a numerical solution of the problem for $N = 2$. The comparison supports the boundary-layer assumptions introduced in the asymptotic analysis.

1. Introduction

The objective of the bounding theory of turbulence is to provide bounds on average properties of statistically stationary turbulent flows. The average properties are regarded as functionals of the turbulent velocity field which can be defined for more general vector fields. The bounds are derived by determining the extremum of the functional among a class of vector fields which includes all statistically stationary solutions of the basic equations of motion. By restricting the fields admitted into competition for the extremum to those which share with the *solutions* an ever greater number of properties one can improve the bounds and bring them into ever closer correspondence with the observed values.

Howard (1963) introduced this approach when he derived upper bounds for the heat transport by convection in a fluid layer heated from below. It was shown later by Busse (1969*a*) that the same approach can be used for a variety of turbulent transport processes. For solenoidal vector fields it was found that the extremalizing field resembled in a number of aspects the structure of the observed turbulent velocity field. The variational problem for the extremalizing fields seems well-posed in a class of solutions of many wavenumbers (multi-α solutions).

An understanding of these solutions and the strongly nonlinear Euler equations which generate them is one object of our study.

Two considerations have motivated the choice of convection in a porous medium as the subject of a detailed study. Although convection processes in porous media have been extensively investigated experimentally, no theory exists for the strongly nonlinear regime. The second consideration is that the Euler equations for the extremum of the heat transport in a porous medium are very similar to those solved by Howard (1963) and Busse (1969*b*). Yet they are simpler and can be analysed in more detail. They represent, possibly, the simplest case in which multi-α solutions with a multiple-boundary-layer structure exist. Since the boundary-layer theory in the previous work is based on a number of assumptions, it is important to verify the assumptions by the comparison with exact analytical or numerical solutions. It is of interest that in the porous case an explicit expression can be obtained for the single-α solution, characterized by a single wavenumber and a single boundary layer. A comparison for solutions with more than one wavenumber is made possible for the first time by the numerical computation of the two-α solution. The results confirm the correctness of the boundary-layer assumptions made in the earlier work.

The paper starts with the derivation of the variational problem in § 2. In § 3 general properties of the multi-α solutions of the Euler–Lagrange equations will be discussed. The derivation of the single-α solution in terms of elliptic integrals is described in § 4. A simplified small amplitude perturbation analysis of steady solutions of the Darcy–Boussinesq equations is also carried out in § 4. Comparison of the perturbation solution and the single-α solution shows that there is a sense in which the single-α bound is the best possible. The general asymptotic boundary-layer analysis for multi-α solutions follows in § 5. The two-α solution, characterized by two successive boundary layers, can be regarded as representative of all the multi-α solutions, since it exhibits all characteristic properties of extremalizing solutions with more than one wavenumber. The numerical analysis of the two-α solution described in § 6 demonstrates the appearance of the boundary-layer structure as the asymptotic case is approached. A comparison with experimental observations is given in § 7.

2. Formulation of the variational problem

The configuration to be considered is an infinitely extended horizontal porous layer filled with fluid and heated from below. The layer has thickness d and is bounded by two parallel plates. The upper plate is kept at a constant temperature T_1 and the lower plate at temperature T_2. To obtain a non-dimensional description of the problem we shall use d, d^2/κ and $(T_2 - T_1)R^{-1}$ as units for length, time and temperature, respectively, κ being the thermal diffusivity of the porous medium and R the Rayleigh number, to be defined below. The Darcy–Boussinesq equations for convection in a porous layer are

$$B(\partial \mathbf{u}/\partial t + \mathbf{u}.\nabla \mathbf{u}) + \nabla p - \mathbf{k}(T - T_1) + \mathbf{u} = 0, \tag{2.1}$$

$$\partial T/\partial t + \mathbf{u}.\nabla T - \nabla^2 T = 0, \tag{2.2}$$

where $\mathbf{k}$ denotes the unit vector in the direction opposite to that of the force of gravity. The equations (2.1) and (2.2) differ from the Boussinesq equations for convection in an ordinary fluid layer only in so far as the frictional force $\nabla^2\mathbf{u}$ is replaced by $-\mathbf{u}$. The solenoidal velocity vector $\mathbf{u}$ is defined according to Darcy's law as an average over the microscale of the porous medium. We shall assume that the microscale is small enough compared with all other scales used in this paper for $\mathbf{u}$ to remain a well-defined quantity. Equations (2.1) and (2.2) were first used by Lapwood (1948) and they are the basic equations for our analysis. It should be noted, however, that the form of the nonlinear inertial term $\mathbf{u}.\nabla\mathbf{u}$ may be inappropriate since $\mathbf{u}$ should be interpreted as the averaged velocity (cf. Irmay 1958). Of the two parameters $R \equiv \gamma g K d(T_2 - T_1)/\nu\kappa$ and $B \equiv \kappa K/d^2\nu$ only the Rayleigh number R will enter the analysis and the bounds derived in this paper will hold independently of the value of B. The constants γ, g, ν and K are the coefficient of thermal expansion, the acceleration of gravity, the kinematic viscosity and the Darcy permeability coefficient, respectively. The thermal diffusivity κ is defined as the thermal conductivity of the fluid–solid mixture divided by the specific heat and the density of the fluid (see § 7). We shall use a Cartesian system of co-ordinates with the z axis in the direction of $\mathbf{k}$ and the origin at the lower boundary. The boundary conditions for the temperature T and the velocity vector $\mathbf{u}$ are

$$\left.\begin{aligned} T = R, \quad \mathbf{k}.\mathbf{u} = 0 \quad \text{at} \quad z = 0, \\ T = 0, \quad \mathbf{k}.\mathbf{u} = 0 \quad \text{at} \quad z = 1. \end{aligned}\right\} \tag{2.3}$$

Since we have used the Darcy constitutive assumption in order to replace $\nabla^2\mathbf{u}$ with $-\mathbf{u}$ in (2.1), we cannot impose boundary conditions on the tangential components of the velocity vector.

The goal of the following analysis is to obtain bounds on the heat transport by convection under stationary conditions. We define this case by assuming that the solutions corresponding to the physically realized convection belong to the class $S(\mathbf{u}, T)$ of statistically stationary solutions. This class consists of all solutions of (2.1) and (2.2) for which (*a*) horizontal averages exist and are bounded and (*b*) horizontal averages are time-independent. Restricting our attention from now on to this class of solutions, we indicate the horizontal average by an overbar. By taking the horizontal average of (2.2) and subtracting it from (2.2) we obtain two equations for T and the fluctuating temperature $\theta \equiv T - \overline{T}$:

$$\overline{\mathbf{u}.\nabla\theta} - d^2\overline{T}/dz^2 = 0, \tag{2.4}$$

$$\partial\theta/\partial t + \mathbf{u}.\nabla\theta - \overline{\mathbf{u}.\nabla\theta} + \mathbf{u}.\nabla\overline{T} - \nabla^2\theta = 0. \tag{2.5}$$

Integration of (2.4) yields, after the boundary conditions (2.3) have been taken into account,

$$d\overline{T}/dz = \overline{w\theta} - \langle w\theta\rangle - R, \tag{2.6}$$

where w is the vertical component of $\mathbf{u}$ and the angular brackets denote the average over the entire layer. By multiplying (2.1) by $\mathbf{u}$ and (2.5) by θ and averaging we obtain

$$\langle|\mathbf{u}|^2\rangle = \langle w\theta\rangle, \tag{2.7}$$

$$\langle|\nabla\theta|^2\rangle + \langle(\overline{w\theta} - \langle w\theta\rangle)^2\rangle = R\langle w\theta\rangle, \tag{2.8}$$

where we have used the relation (2.6) and the identity

$$\langle\overline{w\theta^2}\rangle - \langle w\theta\rangle^2 = \langle(\overline{w\theta} - \langle w\theta\rangle)^2\rangle.$$

The heat transport across the layer is given by the mean temperature gradient at the boundary: $H = R + \langle w\theta\rangle$. The function giving the dependence of H on the Rayleigh number R for the physically realized convection is the one of foremost interest in the problem of porous convection, Since this function cannot be determined except for small values of $\langle w\theta\rangle$, it is important to find bounds on H for given R or vice versa. From (2.7) it is evident that H must be greater than R except in the case of the static solution, when H is equal to R (Westbrook 1969). Though it is physically more natural to start from a fixed value R and find H mathematically, it is more convenient to do the opposite. This path leads, as Howard first showed, to a precisely formulated variational problem of the type which is described below.

In formulating the variational problem it is as well to give the variational functional a homogeneous form. By using the notation $\mu = \langle w\theta\rangle$ we may combine (2.7) and (2.8) into

$$R = \frac{\langle|\mathbf{u}|^2\rangle\langle|\nabla\theta|^2\rangle}{\langle w\theta\rangle^2} + \mu\frac{\langle(\overline{w\theta} - \langle w\theta\rangle)^2\rangle}{\langle w\theta\rangle^2} \equiv \mathscr{F}[\mathbf{u}, \theta; \mu]. \tag{2.9}$$

We next define a class $\mathscr{H}$ of admissible functions and vectors:

$$\mathscr{H} \equiv \{\mathbf{u}, \theta; \nabla.\mathbf{u} = 0, \mathbf{u} = \theta = 0|_{z=0,1}, \overline{u} = \overline{\theta} = 0\}. \tag{2.10a}$$

Among the elements $(\mathbf{u}, \theta) \in \mathscr{H}$ are those which belong to the set $\mathscr{N}$ whose elements satisfy the normalizing conditions

$$\mu = \langle w\theta\rangle, \quad \langle|\mathbf{u}|^2\rangle = \langle w\theta\rangle. \tag{2.10b}$$

Every statistically stationary solution is simultaneously an element of $\mathscr{H}$ and $\mathscr{N}$.

Consider next the variational problem

$$F(\mu) = \min_{\mathscr{H}} \mathscr{F}[\mathbf{u}, \theta; \mu] \tag{2.11}$$

for preassigned values of $\mu \geqslant 0$. Since $\mathscr{F}$ is a homogeneous functional of degree zero we may always renormalize the element $(\tilde{u}, \tilde{\theta})$ which gives $\mathscr{F}$ its minimum value over $\mathscr{H}$, F, so as to satisfy the conditions $\mathscr{N}$. Hence we may obtain a value of F which is unique among elements in $\mathscr{H} + \mathscr{N}$. Since statistically stationary solutions are also elements of $\mathscr{H} + \mathscr{N}$ we have, using (2.9) and (2.11), $R \geqslant F(\mu)$. We may thus conclude that *statistically stationary convection with heat transport μ cannot exist when $R < F(\mu)$.*

The variational problem can be simplified considerably by the introduction of the poloidal (corresponding to χ) and toroidal (corresponding to ψ) decomposition of solenoidal vector fields:

$$\mathbf{u} = \nabla \times (\nabla \times \mathbf{k}\chi) + \nabla \times \mathbf{k}\psi \equiv \mathbf{u}_1 + \mathbf{u}_2.$$

Since $w_2 \equiv 0$ we have

$$w = w_1 = -\Delta_2\chi \equiv -\left(\frac{\partial^2}{\partial x^2} + \frac{\partial^2}{\partial y^2}\right)\chi.$$

It follows from the orthogonality condition $\langle \mathbf{u}_1 . \mathbf{u}_2 \rangle = 0$ that we may write (2.9) as

$$\frac{(\mathscr{F}+\mu)\langle w\theta\rangle^2 - \mu\langle \overline{w\theta}^2\rangle}{\langle |\nabla\theta|^2\rangle} = \langle |\mathbf{u}|^2\rangle = \langle |\mathbf{u}_1|^2 + |\mathbf{u}_2|^2\rangle \geqslant \langle |\mathbf{u}_1|^2\rangle$$

and that the minimum of $\mathscr{F}$ in $\mathscr{H}$ must be taken over fields with $\mathbf{u}_2 = 0$, that is $\psi = 0$. With $\psi = 0$ the Euler equations for χ and θ minimizing $\mathscr{F}$ become

$$\left.\begin{aligned} \langle |\nabla\theta|^2\rangle \nabla^2 w - [(F+\mu)\langle w\theta\rangle - \mu\overline{w\theta}]\,\Delta_2\theta = 0, \\ \langle |\mathbf{k}\times\nabla\nabla\chi|^2\rangle \nabla^2\theta + [(F+\mu)\langle w\theta\rangle - \mu\overline{w\theta}]\, w = 0. \end{aligned}\right\} \tag{2.12}$$

Our problem may now be formulated as: given μ find w, θ and the smallest value of F which satisfy (2.12), the zero-mean condition and the boundary conditions. In the next section we take preliminary steps toward the resolution of this problem.

3. Multi-α solutions

The Euler equations (2.12) admit a large manifold of solutions, each corresponding to a relative extremum of the functional $\mathscr{F}$. We expect to find the minimizing solution among a class of solutions for which the horizontal dependence is characterized by a discrete wavenumber. This is true when $\mu = 0$ and is the hypothesis for the calculation to follow. In the general case we assume

$$\left.\begin{aligned} \chi = \chi^{(N)} \equiv \sum_{n=1}^{N} W_n(z)\,\phi_n(x,y)\,\alpha_n^{-\frac{3}{2}}, \\ \theta = \theta^{(N)} \equiv \sum_{n=1}^{N} \theta_n(z)\,\phi_n(x,y)\,\alpha_n^{-\frac{1}{2}}, \end{aligned}\right\} \tag{3.1}$$

where ϕ_n satisfies the equation $\Delta_2\phi_n = -\alpha_n^2\phi_n$ and the orthogonality condition $\overline{\phi_n\phi_m} = \delta_{nm}$, where δ_{nm} is Kronecker's delta. The functions W_n, θ_n and ϕ_n and the wavenumbers α_n will depend in general on the parameter N. This dependence will be indicated only when it becomes necessary to distinguish between different solutions.

The solutions of the form (3.1), which we shall call multi-α solutions, have a number of interesting properties. We observe that the functional $\mathscr{F}(\mu, \chi^{(N)}, \theta^{(N)})$ is completely symmetric with respect to an interchange of W_n and θ_n. This suggests that the minimum may be found among the smaller class of competitors for which

$$W_n = \theta_n. \tag{3.2}$$

We shall prove this conjecture by adapting the idea of a proof originally given by Howard in a similar situation.

The Euler equations for an extremum of the functional $\mathscr{F}(\mu, \chi^{(N)}, \theta^{(N)})$ can be written in the form

$$\left.\begin{aligned} (D^2-\alpha_n^2)\,W_n + \alpha_n\phi\theta_n = 0, \\ (D^2-\alpha_n^2)\,\theta_n + \alpha_n\phi W_n = 0, \end{aligned}\right\} \tag{3.3}$$

where

$$\phi \equiv F\sum_{\nu}\langle W_\nu\theta_\nu\rangle + \mu\Big(\sum_{\nu}\langle W_\nu\theta_\nu\rangle - \sum_{\nu} W_\nu\theta_\nu\Big)$$

and $D \equiv d/dz$. Here and in the following the summation over the index ν runs from 1 to N unless indicated otherwise.

For mathematical convenience we have replaced the normalization conditions (2.11) by the conditions

$$\sum_\nu \langle W_\nu'^2/\alpha_\nu + \alpha_\nu W_\nu^2 \rangle = \sum_\nu \langle \theta_\nu'^2/\alpha_\nu + \alpha_\nu \theta_\nu^2 \rangle = 1. \tag{3.4}$$

In addition, we can assume without loss of generality that

$$\sum_\nu \langle W_\nu \theta_\nu \rangle > 0. \tag{3.5}$$

In preparation for the proof that $W_n = \theta_n$ we introduce the variables

$$\sigma_n \equiv \tfrac{1}{2}(W_n + \theta_n) \quad \text{and} \quad \tau_n = \tfrac{1}{2}(W_n - \theta_n)$$

and find from (3.3) that

$$(D^2 - \alpha_n^2)\,\sigma_n + \alpha_n \phi \sigma_n = 0, \quad (D^2 - \alpha_n^2)\,\tau_n - \alpha_n \phi \tau_n = 0, \tag{3.6a,b}$$

where ϕ is given in terms of σ_n and τ_n by

$$\phi = (F + \mu) \sum_n \langle \sigma_n^2 - \tau_n^2 \rangle - \mu \sum_n (\sigma_n^2 - \tau_n^2). \tag{3.7}$$

Multiplication of (3.6a) by σ_n yields

$$\frac{1}{2}\frac{d^2}{dz^2}\sigma_n^2 = -\alpha_n \phi \sigma_n^2 + (D\sigma_n)^2 + (\alpha_n \sigma_n)^2,$$

and after summation over all n we obtain

$$\frac{1}{2}\frac{d^2}{dz^2}\sigma^2 = -\phi \sum_n \alpha_n \sigma_n^2 + \sum_n \{(D\sigma_n)^2 + (\alpha_n \sigma_n)^2\} \tag{3.8}$$

and, analogously,

$$\frac{1}{2}\frac{d^2}{dz^2}\tau^2 = +\phi \sum_n \alpha_n \tau_n^2 + \Sigma\{(D\tau_n)^2 + (\alpha_n \tau_n)^2\}, \tag{3.9}$$

where the abbreviation $\sigma^2 = \sum_n \sigma_n^2$ has been used. Equation (3.9) shows that τ^2 cannot have a maximum value in any interval on which $\phi > 0$. Since $\tau^2 = 0$ at $z = 0, 1$ and $\tau^2 \geqslant 0$ we may conclude that

$$\tau^2 = \sum_n \tau_n^2 \equiv 0 \quad \text{if} \quad \phi \geqslant 0 \quad \text{for} \quad -\tfrac{1}{2} \leqslant z \leqslant \tfrac{1}{2}. \tag{3.10}$$

We note that $\phi > 0$ at $z = 0, 1$. To prove $\phi \geqslant 0$ throughout $[-\frac{1}{2}, \frac{1}{2}]$ we show that it is not possible to have $\phi < 0$ on some interior interval $z_1 < z < z_2$ with $\phi = 0$ at z_1 and z_2. Assume that it is possible. Then we find

$$0 \geqslant \frac{d}{dz}\phi = \frac{d}{dz}(\tau^2 - \sigma^2) \quad \text{at} \quad z = z_1,$$

or

$$\left.\frac{d\sigma^2}{dz}\right|_{z=z_1} \geqslant \left.\frac{d\tau^2}{dz}\right|_{z=z_1}, \tag{3.11a}$$

and similarly

$$\left.\frac{d\tau^2}{dz}\right|_{z=z_2} \geqslant \left.\frac{d\sigma^2}{dz}\right|_{z=z_2}. \tag{3.11b}$$

Since $\phi < 0$ in the open interval (z_1, z_2), integration of (3.8) over the closed interval yields

$$\left.\frac{d\sigma^2}{dz}\right|_{z=z_2} > \left.\frac{d\sigma^2}{dz}\right|_{z=z_1}, \tag{3.12}$$

where the inequality is strict because σ^2 and α_n are positive. From (3.11*a*, *b*) and (3.12) we conclude that

$$\left.\frac{d\tau^2}{dz}\right|_{z=z_2} > \left.\frac{d\tau^2}{dz}\right|_{z=z_1}. \tag{3.13}$$

Hence $d\tau^2/dz$ has a strictly positive increase over any interval with $\phi < 0$. Since it cannot decrease over intervals with $\phi \geqslant 0$, as is evident from (3.9), $d\tau^2/dz$ shows a strictly positive increase from $z = 0$ to $z = 1$. Since $\tau = 0$ at $z = 0, 1$ we cannot have $\phi < 0$ and it follows that $\tau^2 = 0$, proving (3.2).

Using (3.2) we rewrite the variational functional (2.9) for the multi-α solutions in the form

$$\mathscr{F}(\mu, \boldsymbol{\theta}^{(N)}, \boldsymbol{\alpha}^{(N)}) = \{[I(\boldsymbol{\alpha}^{(N)}, \boldsymbol{\theta}^{(N)})]^2 + \mu \langle (|\boldsymbol{\theta}^{(N)}|^2 - \langle |\boldsymbol{\theta}^{(N)}|^2 \rangle)^2 \rangle\} \langle |\boldsymbol{\theta}^{(N)}|^2 \rangle^{-2}, \tag{3.14}$$

where

$$I(\boldsymbol{\alpha}^{(N)}, \boldsymbol{\theta}^{(N)}) \equiv \sum_\nu \langle \alpha_\nu^{-1} \theta_\nu'^2 + \alpha_\nu \theta_\nu^2 \rangle.$$

To shorten the notation we have introduced the N-dimensional vector $\boldsymbol{\theta}^{(N)}$, which has the functions $\theta_n(z)$ as its components. Similarly, we have combined the wavenumbers α_n to form the vector $\boldsymbol{\alpha}^{(N)}$. The index (N) will be dropped in the following except when different multi-α solutions have to be distinguished. The minimum of the functional (3.14) for a given N will be denoted by $F_N(\mu)$. The symbol $F(\mu)$ will be reserved for the absolute minimum among the class of minima $F_N(\mu)$. The Euler equations for the minimum $F_N(\mu)$ of the functional (3.14) are

$$\theta_n'' - \alpha_n^2 \theta_n + (\alpha_n / I)\{(F_N + \mu) \langle |\boldsymbol{\theta}|^2 \rangle - \mu |\boldsymbol{\theta}|^2\} \theta_n = 0 \tag{3.15}$$

and the corresponding boundary conditions are

$$\theta_n(0) = \theta_n(1) = 0 \quad \text{for} \quad n = 1, \ldots, N. \tag{3.16}$$

The symmetry of the equations suggests that *the solutions $\theta_n(z)$ are either symmetric or antisymmetric with respect to $z = \frac{1}{2}$*. To prove this we separate the vector $\boldsymbol{\theta}$ into its symmetric and antisymmetric parts:

$$\boldsymbol{\theta} = \boldsymbol{\theta}_s + \boldsymbol{\theta}_a,$$

with $\boldsymbol{\theta}_s \equiv \frac{1}{2}\{\boldsymbol{\theta}(z) + \boldsymbol{\theta}(1-z)\}$ and $\boldsymbol{\theta}_a = \frac{1}{2}\{\boldsymbol{\theta}(z) - \boldsymbol{\theta}(1-z)\}$. The functional (3.14) obviously satisfies the relation

$$\mathscr{F}(\mu, \boldsymbol{\theta}, \boldsymbol{\alpha}) \geqslant \hat{\mathscr{F}}(\mu, \boldsymbol{\theta}_s, \boldsymbol{\theta}_a, \boldsymbol{\alpha})$$

with

$$\hat{\mathscr{F}} \equiv \{[I(\boldsymbol{\alpha}, \boldsymbol{\theta}_s) + I(\boldsymbol{\alpha}, \boldsymbol{\theta}_a)]^2 + \mu \langle (|\boldsymbol{\theta}_s|^2 + |\boldsymbol{\theta}_a|^2 - \langle |\boldsymbol{\theta}_s|^2 + |\boldsymbol{\theta}_a|^2 \rangle)^2 \rangle\} \times \langle |\boldsymbol{\theta}_s|^2 + |\boldsymbol{\theta}_a|^2 \rangle^{-2} \tag{3.17}$$

since $\hat{\mathscr{F}}$ is the same as expression (3.14) except that the positive term

$$4\mu\langle(\boldsymbol{\theta}_s.\boldsymbol{\theta}_a)^2\rangle\langle|\boldsymbol{\theta}_s|^2+|\boldsymbol{\theta}_a|^2\rangle^{-2} \tag{3.18}$$

has been neglected. We consider $\hat{\mathscr{F}}$ as a functional of the symmetric vector $\boldsymbol{\theta}_s$ and the antisymmetric vector $\boldsymbol{\theta}_a$, and obtain as necessary conditions for the minimum $\hat{F}(\mu)$ of $\hat{\mathscr{F}}$ the Euler equations

$$\left.\begin{aligned}\theta''_{sn}-\alpha_n^2\theta_{sn}+\alpha_n\phi\theta_{sn}&=0,\\ \theta''_{an}-a_n^2\theta_{an}+\alpha_n\phi\theta_{an}&=0,\end{aligned}\right\} \tag{3.19}$$

with

$$\phi\equiv\{(\hat{F}_N+\mu)\langle|\boldsymbol{\theta}_s|^2+|\boldsymbol{\theta}_a|^2\rangle-\mu(|\boldsymbol{\theta}_s|^2+|\boldsymbol{\theta}_a|^2)\}[I(\boldsymbol{\alpha},\boldsymbol{\theta}_s)+I(\boldsymbol{\alpha},\boldsymbol{\theta}_a)]^{-1}.$$

From (3.19) we obtain

$$\theta''_{sn}\theta_{na}-\theta''_{an}\theta_{sn}=0$$

and by integration of this relation over the interval $0\leqslant z\leqslant\frac{1}{2}$ we find that

$$\theta'_{an}(\tfrac{1}{2})\,\theta_{sn}(\tfrac{1}{2})=0, \tag{3.20}$$

since θ_{sn} as well θ_{an} vanishes at the boundaries $z=0,1$. Relation (3.20) requires that either θ_{an} or θ_{sn} vanishes together with its derivative at $z=\frac{1}{2}$ since by definition $\theta_{an}(\frac{1}{2})=\theta'_{sn}(\frac{1}{2})=0$. Because ϕ is non-singular, however, any solution of (3.19) which vanishes together with its derivative at some point must vanish identically. Hence we can conclude that the vectors $\boldsymbol{\theta}_s$ and $\boldsymbol{\theta}_a$ minimizing $\hat{\mathscr{F}}$ have the property

$$\boldsymbol{\theta}_s.\boldsymbol{\theta}_a\equiv 0. \tag{3.21}$$

Since the functionals $\mathscr{F}$ and $\hat{\mathscr{F}}$ become identical for vectors $\boldsymbol{\theta}_s$ and $\boldsymbol{\theta}_a$ with the property (3.21), the vectors $\boldsymbol{\theta}_s$ and $\boldsymbol{\theta}_a$ minimizing $\hat{\mathscr{F}}$ must also minimize $\mathscr{F}$. This proves the conjecture that the minimizing solutions θ_n of the Euler equations (3.15) are either symmetric or antisymmetric with respect to $z=\frac{1}{2}$.

It is worth pointing out some further properties of the multi-α solutions. Without loss of generality we can assume that all *wavenumbers α_n are different.* If two or more wavenumbers are equal the problem can always be reduced to a case in which all wavenumbers are equal, as the following consideration shows. Suppose that $\alpha_1=\alpha_2$. In this case it is readily seen that the corresponding solutions θ_1 and θ_2 of (3.15) satisfy the relation

$$\theta''_1\theta_2-\theta''_2\theta_1=0,$$

which by integration and use of (3.16) yields $\theta'_1\theta_2-\theta'_2\theta_1=0$ or $(\theta_2/\theta_1)'=0$ in any interval with non-vanishing θ_1. Hence θ_2 must be a multiple of θ_1, say $\theta_2=\gamma\theta_1$. Then the vector $\boldsymbol{\theta}^{(N)}$ of N functions can be reduced to a vector of $N-1$ functions by neglecting θ_2 and α_2 and replacing θ_1 by $\theta_1(1+\gamma^2)^{\frac{1}{2}}$.

The solutions of (3.15) are characterized by two orthogonality relations. The first relation is obtained by multiplying the equation for θ_n by $\alpha_n^{-1}\theta_m$ and the equation for θ_m by $\alpha_m^{-1}\theta_n$. Averaging the equations and subtracting them yields after integration by parts

$$\frac{\alpha_m-\alpha_n}{\alpha_m\alpha_n}\{\langle\theta'_m\theta'_n\rangle-\alpha_m\alpha_n\langle\theta_m\theta_n\rangle\}=0.$$

Since $\alpha_m \neq \alpha_n$ we have

$$\langle \theta'_m \theta'_n \rangle - \alpha_m \alpha_n \langle \theta_m \theta_n \rangle = 0. \tag{3.22}$$

The other relation is obtained by the same process without using the factors α_n^{-1} and α_m^{-1}, respectively:

$$\langle \{(F_N + \mu)\langle |\boldsymbol{\theta}|^2 \rangle - \mu |\boldsymbol{\theta}|^2 - (\alpha_n + \alpha_m) I\} \theta_n \theta_m \rangle = 0. \tag{3.23}$$

We call (3.22) and (3.23) orthogonality relations although θ_m and θ_n are not necessarily orthogonal functions in the usual sense.

The wavenumber α_n can be determined by minimizing the functional (3.14) as a function of $\boldsymbol{\alpha}$. The condition $\partial \mathscr{F}(\mu, \boldsymbol{\theta}, \boldsymbol{\alpha})/\partial \alpha_m = 0$ yields the wavenumber formula

$$\alpha_n^2 = \langle \theta_n'^2 \rangle / \langle \theta_n^2 \rangle. \tag{3.24}$$

In differentiating the functional we have assumed that the functions θ_n satisfy the Euler equations. Hence the implicit dependence of the functional on α_n through $\theta_n(\boldsymbol{\alpha})$ can be neglected since the function is stationary with respect to variations of the function $\theta_n(\boldsymbol{\alpha})$. Formula (3.24) shows that relation (3.22) includes the case $m = n$ if the minimizing value of the wavenumbers are used. The interpretation of (3.24) is that the dissipation $\langle |\theta'_n|^2 \rangle$ associated with the vertical scale is equal for each function θ_n to the dissipation $\alpha_n^2 \langle \theta_n^2 \rangle$ associated with the horizontal scale.

Finally, we note that the multi-α solutions have an energy integral which may be written as

$$I \sum_{n=1}^{N} \left(\frac{\theta_n'^2}{\alpha_n} - \alpha_n \theta_n^2 \right) + (F_N + \mu)\langle |\boldsymbol{\theta}|^2 \rangle (|\boldsymbol{\theta}|^2 - \langle |\boldsymbol{\theta}|^2 \rangle) - \tfrac{1}{2}\mu(|\boldsymbol{\theta}|^4 - \langle |\boldsymbol{\theta}|^4 \rangle) = I \left\langle \sum_{n=1}^{N} \frac{\theta_n'^2}{\alpha_n} - \alpha_n \theta_n^2 \right\rangle.$$

When the α_n have their optimal values, given by (3.24), the right-hand side of this equation vanishes.

4. The single-α solution and the situation for small μ

When $\mu = 0$ we must solve the linear problem

$$\theta_m'' - \alpha_m^2 \theta_m + F_N \frac{\alpha_m \langle |\boldsymbol{\theta}|^2 \rangle}{I} \theta_m = 0, \tag{4.1}$$

with $\theta_m = 0$ at $z = 0, 1$. From (4.1) we see that all even derivatives of $\theta_m(z)$ vanish at the boundary. Hence $\theta_m(z)$ can be developed as $\theta_m(z) = \sum_{n=1}^{\infty} A_{mn} \sin n\pi z$, which together with (4.1) implies that

$$F_N = \frac{I}{\langle |\boldsymbol{\theta}|^2 \rangle} \left\{ \frac{n^2 \pi^2}{\alpha_m} + \alpha_m \right\}. \tag{4.2}$$

On the other hand, on multiplying (4.1) by θ_m integrating and summing over m we find that

$$F_N = I^2 / \langle |\boldsymbol{\theta}|^2 \rangle^2. \tag{4.3}$$

Hence the minimum of $F_N^{\frac{1}{2}} = n^2\pi^2/\alpha_m + \alpha_m$ over α_m is $F_N(n) = 4n^2\pi^2$ for $\alpha_m = n\pi$. The expression $F_N(n)$ reaches its lowest value $F_N = 4\pi^2$ for $n = 1$, $\alpha_m = \pi$ and $\theta_m(z) = A_m \sin \pi z$. The minimizing solutions $\theta_m(z)$ are therefore identical apart from a multiplicative constant. The number N of different horizontal scales α_m^{-1} required for minimizing F_N when $\mu = 0$ is just one: $N(\mu) = 1$ when $\mu = 0$ and $\min_N F_N = F_1$.

Now we shall seek the minimum $F_1(\mu)$ of $\mathscr{F}_1[\theta; a, \mu]$ over functions with a single wavenumber α. More than one wavenumber is required to minimize $\mathscr{F}$ when μ is large. When $N = 1$ we may write (3.25) as

$$I_1((D\theta)^2/\alpha - \alpha\theta^2) + (F_1 + \mu)\langle\theta^2\rangle\theta^2 - \tfrac{1}{2}\mu\theta^4 = A = \text{constant}, \tag{4.4}$$

where

$$I_1 = \langle(D\theta)^2/\alpha + \alpha\theta^2\rangle$$

and, with θ normalized so that the maximum value of θ is one,

$$A = -\alpha I_1 + (F_1 + \mu)\langle\theta^2\rangle - \tfrac{1}{2}\mu. \tag{4.5}$$

The wavenumber α is to have the value given by $\alpha^2 = \langle(D\theta)^2\rangle/\langle\theta^2\rangle$ from (3.24). This implies that

$$I_1/\alpha = 2\langle\theta^2\rangle, \quad \alpha I_1 = 2\langle(D\theta)^2\rangle. \tag{4.6}$$

Elimination of α in (4.4) with the constants as given in (4.5) and (4.6) gives

$$(D\theta)^2 = \lambda(1-\theta^2)(1-k^2\theta^2), \tag{4.7}$$

where $k^2 = \mu/\{2(F_1+\mu)\langle\theta^2\rangle - 4\langle(D\theta)^2\rangle - \mu\}$ and $\lambda = \mu/4k^2\langle\theta^2\rangle$.

To write the required result we employ the complete elliptic integrals $K(k^2)$ and $D(k^2)$. Here k lies in the range $[0, 1]$. One finds by integration of (4.7) that

$$\lambda^{\frac{1}{2}} = 2nK(k^2), \tag{4.8}$$

where n is the number of half-periods of θ on $0 \leqslant z \leqslant 1$,

$$\langle\theta^2\rangle = 2n\int_0^1 W^2 \frac{dz}{d\theta}d\theta = \frac{2n}{\lambda^{\frac{1}{2}}}D(k^2) = D(k^2)/K(k^2) \tag{4.9}$$

and

$$\langle(D\theta)^2\rangle = 2n\lambda\int_0^1 (1-\theta^2)(1-k^2\theta^2)\frac{dz}{d\theta}d\theta = 2n\lambda^{\frac{1}{2}}\int_0^1 [(1-\theta^2)(1-k^2\theta^2)]^{\frac{1}{2}}d\theta.$$

The last expression may be reduced by a standard transformation for elliptic integrals (Hancock 1958, p. 63) to

$$\langle(D\theta)^2\rangle = 4n^2K[\tfrac{2}{3}K - \tfrac{1}{3}(k^2+1)D]. \tag{4.10}$$

Using the expressions (4.8), (4.9) and (4.10) in the definition of k^2 and λ, we have

$$F_1 = \tfrac{16}{3}n^2\{(k^2+1)K^2 + K^3/D - 3k^2DK\} \tag{4.11}$$

and

$$\mu = 16n^2k^2DK. \tag{4.12}$$

Equations (4.11) and (4.12) give the value $F_1(\mu, n)$ parametrically. The smallest value $F_1(\mu)$ of $F_1(\mu, n)$ is taken on for $n = 1$.

We have therefore shown that among functions with a single wavenumber (chosen optimally) the minimum value $F_1(\mu)$ of the functional $\mathscr{F}_1$ is given parametrically by (4.11) and (4.12) with $n = 1$. Statistically stationary convection

with heat transport μ and a single overall wavenumber cannot exist when $R < F_1(\mu)$. The curve $F_1(\mu)$ for $N = 1$ is given in figure 6 below. Evaluation of (4.11) and (4.12) in the asymptotic case of large μ yields $F_1(\mu) = \frac{16}{3}\mu^{\frac{1}{2}}$. This result can also be obtained directly by constructing a boundary-layer analysis similar to that given by Howard (1963). The boundary-layer thickness is proportional to $\mu^{-\frac{1}{2}}$. Since this case is included in the more general analysis of § 5, we shall not pursue this problem further at this point.

When $\mu = 0$, $k^2 = 0$ and one finds that $F_1 = 4\pi^2$. The slope of tbe heat transport curve at the point $\mu = 0$ is

$$\frac{dF_1}{d\mu} = \frac{\langle(\theta^2 - \langle\theta^2\rangle)^2\rangle}{\langle\theta^2\rangle} = \frac{1}{2}. \tag{4.13}$$

We shall use this result to show the following. *Of all the small statistically stationary solutions of the Darcy–Boussinesq equations in the case $B = 0$, two-dimensional rolls maximize the heat transport. Moreover, the values*

$$F_1(0) = 4\pi^2, \quad dF_1(0)/d\mu = \tfrac{1}{2} \tag{4.14}$$

are the best possible.

The demonstration consists of displaying an actual solution of the nonlinear convection problem with the asserted properties. Consider the problem posed by (2.1) and (2.2) in the case $B = 0$. Equation (2.1) shows that $\mathbf{k}.\nabla\times\mathbf{u} = 0$. Hence the solenoidal field $\mathbf{u}$ can be written as a poloidal vector field:

$$\mathbf{u} = -\nabla\times(\nabla\times\mathbf{k}\hat{\chi}) \equiv \boldsymbol{\delta}\hat{\chi}. \tag{4.15}$$

On forming the vertical component of the curl curl of (2.1) we find

$$\Delta_2(\nabla^2\hat{\chi} + T - T_1) = 0. \tag{4.16}$$

Because $\mathbf{u}$ is periodic, or almost periodic, with zero mean and because T is bounded, the integration of (4.16) with respect to the horizontal co-ordinates yields

$$\nabla^2\hat{\chi} + T - T_1 = f(z),$$

where $f(z)$ is an arbitrary function of z. We notice that an arbitrary function $g(z)$ can be added to $\hat{\chi}$ without changing $\mathbf{u}$. We use this freedom in the definition (4.15) to choose $g(z)$ such that

$$\nabla^2\hat{\chi} + T = T_1 + R(1-z). \tag{4.17}$$

Since the right-hand side in this relation represents the temperature distribution in the static case, $\mathbf{u} = 0$, $-\nabla^2\hat{\chi}$ describes the deviation of the temperature from the static distribution. Using (4.17) to eliminate T from (2.2), we obtain

$$\left(\nabla^2 - \frac{\partial}{\partial t}\right)\nabla^2\hat{\chi} + R\Delta_2\hat{\chi} = \boldsymbol{\delta}\hat{\chi}.\nabla\nabla^2\hat{\chi}, \tag{4.18}$$

which has to be solved subject to the boundary conditions

$$\hat{\chi} = \nabla^2\hat{\chi} = 0 \quad \text{at} \quad z = 0, 1. \tag{4.19}$$

We shall construct a steady solution of (4.18) and (4.19) as an analytic perturbation in the Nusselt number Nu, which is defined as the ratio of the total heat transport divided by the heat transport in the static state:

$$Nu = 1+\frac{\langle wT\rangle}{R} = 1+\frac{\langle \Delta_2\hat{\chi}\nabla^2\hat{\chi}\rangle}{R}.$$

We set $\hat{\chi} = \epsilon\chi$, where $\epsilon^2 = Nu-1$. Then we have to solve

$$\nabla^4\chi + R\Delta_2\chi = \epsilon\boldsymbol{\delta}\chi\,.\,\nabla\nabla^2\chi, \tag{4.20}$$

$$\chi = \nabla^2\chi = 0 \quad \text{at} \quad z = 0{\cdot}1.$$

for functions χ of norm

$$\langle\nabla^2\chi\Delta_2\chi\rangle = R. \tag{4.21}$$

We seek the solutions $\chi(x,y,z,\epsilon)$ and $R(\epsilon)$ of (4.20) and (4.21) as a Taylor series in ϵ. For the first three Taylor coefficients we have to solve

$$\left.\begin{aligned}\nabla^4\chi^{(0)} + R^{(0)}\Delta_2\chi^{(0)} &= 0,\\ \langle\nabla^2\chi^{0)}\Delta_2\chi^{(0)}\rangle &= R^{(0)};\end{aligned}\right\} \tag{4.22}$$

$$\left.\begin{aligned}\nabla^4\chi^{(1)} + R^{(0)}\Delta_2\chi^{(1)} + R^{(1)}\Delta_2\chi^{(0)} &= \boldsymbol{\delta}\chi^{(0)}\,.\,\nabla\nabla^2\chi^{(0)},\\ \langle\nabla^2\chi^{(1)}\Delta_2\chi^{(0)} + \nabla^2\chi^{(0)}\Delta_2\chi^{(1)}\rangle &= R^{(1)};\end{aligned}\right\} \tag{4.23}$$

and

$$\nabla^4\chi^{(2)} + R^{(0)}\Delta_2\chi^{(2)} + 2R^{(1)}\Delta_2\chi^{(1)} + R^{(2)}\Delta_2\chi^{(0)} = 2\{\boldsymbol{\delta}\chi^{(0)}\,.\,\nabla\nabla^2\chi^{(1)} + \boldsymbol{\delta}\chi^{(1)}\,.\,\nabla\nabla^2\chi^{(0)}\}. \tag{4.24}$$

Of course, $\chi^{(n)} = \nabla^2\chi^{(n)} = 0$ at $z = 0, 1$. The solution of (4.22) which is to be perturbed is

$$\chi^{(0)} = (8^{\frac{1}{2}}/\pi)\sin\pi z\cos\pi x, \quad R^{(0)} = 4\pi^2. \tag{4.25}$$

The values $R^{(1)}$ and $R^{(2)}$ are determined, respectively, by solvability conditions which must be applied on the right-hand sides of (4.23) and (4.24):

$$R^{(1)}\langle\nabla^2\chi^{(0)}\Delta_2\chi^{(0)}\rangle = \langle\nabla^2\chi^{(0)}\boldsymbol{\delta}\chi^{(0)}\,.\,\nabla\nabla^2\chi^{(0)}\rangle \tag{4.26}$$

and

$$\tfrac{1}{2}R^{(2)}\langle\nabla^2\chi^{(0)}\Delta_2\chi^{(0)}\rangle = \langle\nabla^2\chi^{(0)}\boldsymbol{\delta}\chi^{(0)}\,.\,\nabla\nabla^2\chi^{(1)}\rangle + \langle\nabla^2\chi^{(0)}\boldsymbol{\delta}\chi^{(1)}\,.\,\nabla\nabla^2\chi^{(0)}\rangle. \tag{4·27}$$

The right-hand side of (4.26) and the second term on the right-hand side of (4.27) integrate to zero; so

$$\langle\nabla^2\chi^{(0)}\boldsymbol{\delta}\chi^{(1)}\,.\,\nabla\nabla^2\chi^{(0)}\rangle = \tfrac{1}{2}\langle\boldsymbol{\delta}\chi^{(1)}\,.\,\nabla(\nabla^2\chi^{(0)})^2\rangle = \langle\nabla\,.\,\boldsymbol{\delta}\chi^{(1)}(\nabla^2\chi^{(0)})^2\rangle = 0.$$

Hence

$$R^{(1)} = 0.$$

The evaluation of the right-hand side of (4.23),

$$\boldsymbol{\delta}\chi^{(0)}\,.\,\nabla\nabla^2\chi^{(0)} = -8\pi^3\sin 2\pi z,$$

shows that

$$\chi^{(1)} = (-1/2\pi)\sin 2\pi z$$

is a solution of (4.21) which satisfies all required the conditions. Next, one finds from (4.27) that

$$4\pi^2R^{(2)} = -4\pi^2\langle\chi^{(0)2}d^3\chi^{(1)}/dz^3\rangle = 16\pi^4.$$

Hence $$R(\epsilon) = 4\pi^2(1 + \tfrac{1}{2}\epsilon^2 + \ldots)$$

and $$dR(\epsilon)/d\epsilon^2 = dR/dNu = 2\pi^2.$$

Since $\epsilon^2 R = \langle wT \rangle = \mu$ it follows that $dR/d\mu = \frac{1}{2}$ at $\mu = 0$.

Summarizing the results, we have found that roll convection exists for small μ in the case $B = 0$ with the following dependence of the Rayleigh number on the convective heat transport μ:

$$R(\mu) = 4\pi^2 + \tfrac{1}{2}\mu + O(\mu^2).$$

We have also found, see (4.13), that

$$F_1(\mu) = 4\pi^2 + \tfrac{1}{2}\mu + O(\mu^2).$$

Recall that statistically stationary convection cannot exist when

$$R < F(\mu) = \min_N F_N(\mu) \leqslant F_1(\mu).$$

Hence we have for small enough μ

$$F(\mu) = 4\pi^2 + \tfrac{1}{2}\mu + O(\mu^2).$$

This proves that at small enough μ the single-α bounding solution gives the same heat transport as an exact steady solution in the case $B = 0$.

5. Boundary-layer analysis of multi-α solutions

No explicit solutions of (3.15) are known for $N > 1$. However, when μ is very large we may anticipate that the solution with many wavenumbers, like the single-α solution given in § 4, has a boundary-layer structure. It is clear already from the form of $\mathscr{F}_N$ expressed in (3.14) that when $\mu \to \infty$ the quantity

$$\mu \langle (|\boldsymbol{\theta}|^2 - \langle |\boldsymbol{\theta}|^2 \rangle)^2 \rangle$$

can be bounded only if $|\boldsymbol{\theta}|^2 \to \langle |\boldsymbol{\theta}|^2 \rangle$ over most of the domain $0 \leqslant z \leqslant 1$ of $\boldsymbol{\theta}(z)$. By adopting, for convenience, the normalization

$$\langle |\theta|^2 \rangle = 1 \tag{5.1a}$$

we see $|\boldsymbol{\theta}(z)| \to 1$ everywhere except in boundary layers, in which $|\boldsymbol{\theta}(z)|$ drops to its zero value at $z = 0, 1$.

For the single-α solution the structure of the boundary layer is determined from the requirement that $\mathscr{F}_1$ be a minimum. This requirement can only be satisfied when the small boundary layer in which θ^2 drops from its interior unit value is large enough for the contributions of the large derivatives to I^2 to be of the same order ($\mu^{\frac{1}{2}}$) as $\mu \langle (1 - \theta^2)^2 \rangle$.

The same sort of minimizing balance can be anticipated in the multi-α case. Here again we must have

$$|\boldsymbol{\theta}|^2 \approx 1 \tag{5.1b}$$

in the interior. To prevent the terms with derivatives in I^2 from growing more sharply than $\mu \langle (1 - |\boldsymbol{\theta}|^2)^2 \rangle$ the solution will develop a boundary layer for $|\boldsymbol{\theta}|^2$ of order μ^{-r_N}, where r_N is a positive number to be determined.

The difference between the multi-α solution and the single-α solution is just this: the presence of the many different functions and wavenumbers allows for the

development of boundary layers within boundary layers; indeed our formal calculation shows that the solution does develop a nested sequence of N boundary layers in which the sharp rise of θ_n^2 takes place in an interval of the same order (in μ) as the slow fall of the function θ_{n+1}^2. This process has the overall effect of allowing one to extend closer to the boundaries the region on which (5.1) holds while, at the same time, holding the dissipation integrals I^2 to within the same order of μ^{1-r_N} as the term $\mu\langle(1-|\theta|^2)^2\rangle$. It is the presence of the different horizontal scales α_n^{-1} which moderates the increase of the dissipation I^2. Indeed inspection of (3.14) shows that I (and $\mathscr{F}_N$) is minimized when the horizontal scale α_n^{-1} equals the vertical scale of the functions θ_n. Hence we know that the functions θ_n^2 with the steepest boundary layers will also have the smallest horizontal scales α_n^{-1}.

In view of the foregoing discussion it seems plausible to postulate that each function $\theta_n^2(z)$ has its own boundary layer. The boundary layer for θ_N^2 is closest to the wall and has a steep rise of order μ^{-r_N}. The function θ_{N-1}^2 also has a boundary layer but here the rise of θ_{N-1}^2 is less sharp and is of $O(\mu^{-r_{N-1}})$, where $r_{N-1} < r_N$. Unlike the boundary-layer solution for the single-α case one cannot anticipate that θ_N with $N > 1$ will tend to one in the interior. If this were the case one could not satisfy (5.1) with non-zero interior values for the other functions θ_n. Moreover, the contribution $\alpha_N\langle\theta_N^2\rangle$ has to be kept small because of the relatively large value of α_N. Hence it is plausible to suppose that θ_N^2 first rises and then falls to zero. It is clear from what we anticipate for the sizes μ^{-r_N} and $\mu^{-r_{N-1}}$ of the two layers closest to the wall that, as $\mu \to \infty$, θ_N^2 may experience a very rapid rise on an interval of order μ^{-r_N} on which θ_{N-1} is barely different from zero, and a relatively gentle fall to zero an interval of order $\mu^{-r_{N-1}}$ on which θ_{N-1} is still rising rapidly relative to the rate of its own subsequent gentle decline in the layer of $O(\mu^{-r_{N-2}})$. The same sharp rise followed by gentle fall is anticipated of the sequence $\theta_N^2, \theta_{N-1}^2, \ldots, \theta_n^2, \theta_{n-1}^2, \ldots$ until the actually rapid but relatively (to θ_2^2) slow rise of θ_1^2 to its interior value $\theta_1^2 \cong 1$ is complete.

We shall now show how the description of the multi-α solution for large μ just given does arise from formal analysis. The hypothesis whose consistency is being tested is that θ_n rises in the nth boundary layer and falls to zero in the $(n-1)$th boundary layer. Hence, each of the functions differs from zero essentially only in two subsequent boundary layers and it is convenient to separate the rising and falling parts. Thus we let

$$\theta_n(z) = \begin{cases} \hat{\theta}_n(\zeta_n) & \text{for} \quad z = O(\mu^{-r_n}), \\ \tilde{\theta}_n(\zeta_{n-1}) & \text{for} \quad z = O(\mu^{-r_{n-1}}), \end{cases} \tag{5.2}$$

where

$$n = 1, \ldots, N, \quad r_n > r_{n-1} \quad \text{and} \quad \zeta_n = z\mu^{r_n} \tag{5.3}$$

is the nth boundary layer co-ordinate. In the limit $\mu \to \infty$ the relations

$$\hat{\theta}_n^2 + \tilde{\theta}_{n+1}^2 = 1 \quad \text{for} \quad z = O(\mu^{-r_n}) \quad (0 \leqslant n < N) \tag{5.4}$$

and

$$\tilde{\theta}_1^2 = 1 \quad \text{for} \quad z = O(\mu^{-r_0}) \quad r_0 = 0 \tag{5.5}$$

are implied by (5.1b) and (5.2). It is this feature which allows one to satisfy (5.1b) close to the wall. Only in the Nth layer is $1 - \theta_N^2 > 0$ when $\mu \to \infty$.

We note that when ζ_n is fixed and $\mu \to \infty$

$$\zeta_{n-1} = \zeta_n \mu^{r_{n-1}-r_n} \to 0.$$

Hence we must have

$$\left.\begin{aligned} \hat{\theta}_n(0) = 0, \quad \hat{\theta}_n(\infty) = 1 \quad \text{for} \quad n = 1, \ldots, N, \\ \tilde{\theta}_n(0) = 1, \quad \tilde{\theta}_n(\infty) = 0 \quad \text{for} \quad n = 2, \ldots, N. \end{aligned}\right\} \tag{5.6}$$

Since the problem is symmetric with respect to the two boundaries, we assume that the same description holds for the boundary layer at $z = 1$ with $1 - z$ replacing z in the definitions (5.2)–(5.4).

Returning now to the expression (3.24) for the best α_n (5.2) and (5.3) we find that

$$\alpha_n^2 = \mu^{r_n - r_{n-1}} b_n^2, \tag{5.7}$$

where

$$b_n^2 = \int_0^\infty \hat{\theta}_n'^2 d\zeta_n \Big/ \int_0^\infty (1 - \hat{\theta}_n^2)\, d\zeta_{n-1}, \quad b_1^2 = 2\int_0^\infty \hat{\theta}_1'^2 d\zeta_1 \tag{5.8}$$

are independent of μ at large μ. Here, the factor 2 arises from the fact that there are two boundary layers, one on each wall. We have eliminated

$$\tilde{\theta}_n^2(\zeta_{n-1}) = 1 - \hat{\theta}_{n-1}^2(\zeta_{n-1})$$

by using (5.5).

To determine the exponents we insert (5.3)–(5.7) into (3.14), let $\mu \to \infty$ and use (5.4) and (5.5) to eliminate $\tilde{\theta}_m^2 (m = 1, \ldots, N)$. We find that

$$\mathscr{F}_N[\theta; \alpha, \mu] = \left\{ \mu^{\frac{1}{2}r_1} b_1 + \frac{2}{b_1}\int_0^\infty \theta'^2 d\zeta_1 + 2\sum_{m=2}^{N} \mu^{\frac{1}{2}(r_m - r_{m-1})} \left(\frac{1}{b_m}\int_0^\infty \theta_m'^2 d\zeta_m \right.\right.$$
$$\left.\left. + b_m \int_0^\infty (1 - \theta_{m-1}^2)\, d\zeta_{m-1} \right) \right\}^2 + 2\mu^{1-r_N} \int_0^\infty (1 - \theta_N^2)^2 d\zeta_N. \tag{5.9}$$

Differentiation of (5.9) with respect to the parameters r_m shows that a minimum can be reached only if all exponents of μ in the terms contributing additively to the right-hand side of (5.9) are equal:

$$1 - r_N = r_N - r_{N-1} = \ldots r_2 - r_1 = r_1.$$

This relation leads to the solution

$$r_m = m/(N+1) \quad \text{for} \quad m = 1, \ldots, N. \tag{5.10}$$

Now, on using (5.10) in (5.9) we have

$$\mathscr{F}_N = \mu^{1/(N+1)} \left\{ \hat{I}^2 + 2\int_0^\infty (1 - \hat{\theta}_N^2)^2 d\zeta_N \right\}, \tag{5.11}$$

where

$$\hat{I} = b_1 + \frac{2}{b_N}\int_0^\infty \hat{\theta}_N'^2 d\zeta_N + 2\sum_{m=1}^{N-1} \int_0^\infty \left[\frac{\hat{\theta}_m'^2}{b_m} + b_{m+1}(1 - \hat{\theta}_m^2) \right] d\zeta_m.$$

The minimum of (5.11) is found for functions which satisfy the Euler equations†

$$\hat{\theta}_m'' + b_m b_{m+1} \hat{\theta}_m = 0 \quad (m = 1, \ldots, N-1), \tag{5.12a}$$

† These equations can also be derived by introducing the boundary-layer assumptions in (3.15). This approach was used in the treatment of the analogous problem of ordinary convection by Busse (1969*b*).

and $$(\hat{I}/b_N)\,\hat{\theta}_N'' + (1-\hat{\theta}_N^2)\,\hat{\theta}_N = 0 \tag{5.12b}$$

subject to the conditions (5.6). The best values of b_m are given by (5.8).

A continuously differentiable solution of (5.12a, b) and (5.6) is given by

$$\hat{\theta}_n = \begin{cases} \pm \sin (b_n b_{n+1})^{\frac{1}{2}} \zeta_n & \text{for} \quad 0 \leqslant \zeta_n \leqslant \pi/2(b_n b_{n+1})^{\frac{1}{2}}, \\ \pm 1 & \text{for} \quad \pi/2(b_n b_{n+1})^{\frac{1}{2}} \leqslant \zeta_n, \end{cases} \tag{5.13}$$

$$\hat{\theta}_N = \pm \tanh \{(\tfrac{1}{2} b_N \hat{I}^{-1})^{\frac{1}{2}} \zeta_N\}. \tag{5.14}$$

Note that the signs of the functions $\hat{\theta}_n$ and $\tilde{\theta}_n$ remain undetermined. This corresponds to the property that $\theta_n(z)$ is either symmetric or antisymmetric. Hence the representations of $\theta_n(z)$ at the two boundaries may have opposite signs. Only when lower order terms, neglected in this approximation, are taken into account can the question of symmetry be decided.

We next calculate $\hat{I}$, b_n and F_N. Using (5.13) and (5.14) we find that

$$\hat{I} = 2 \sum_{n=2}^{N-1} \frac{\pi}{2} \left(\frac{b_{n+1}}{b_n}\right)^{\frac{1}{2}} + b_1 + \tfrac{4}{3}(2 b_N \hat{I})^{-\frac{1}{2}}.$$

The parameters b_n, $n = 1, \ldots, N$, can be determined either from relation (5.8) or by minimizing the functional (5.1) as a function of the b_n. In both cases we arrive at equations of the form

$$1 - \frac{\pi}{2b_1}\left(\frac{b_2}{b_1}\right)^{\frac{1}{2}} = 0,$$

$$\frac{\pi}{2b_n}\left\{\left(\frac{b_n}{b_{n-1}}\right)^{\frac{1}{2}} - \left(\frac{b_{n+1}}{b_n}\right)^{\frac{1}{2}}\right\} = 0 \quad \text{for} \quad n = 1, \ldots, N-1,$$

$$2\frac{\partial \hat{I}}{\partial b_N}(1 + \tfrac{2}{3}(2b_N \hat{I})^{-\frac{1}{2}}) - \tfrac{2}{3}(2b_N \hat{I})^{\frac{1}{2}} b_N^{-2} = 0,$$

which yield the solutions

$$b_n = \frac{\pi}{2}\left(\frac{8}{3\pi^2\sqrt{N}}\right)^{(2n-1)/(N+1)} \quad \text{for} \quad n = 1, \ldots, N,$$

$$\hat{I} = 2Nb_1.$$

The final expression for $F_N(\mu)$ is

$$F_N(\mu) = \mu^{1/(N+1)}\,\hat{F}\,(N) = \mu^{1/(N+1)} N(N+1)\,4b_1^2 = N(N+1)\,\pi^2 (64\mu/9\pi^4 N)^{1/(N+1)}. \tag{5.15}$$

It is of interest to calculate the thicknesses of the boundary layer of the minimizing N-α solution. We define the characteristic thickness $z = \delta_n$ by the property that the arguments of the sin-function and the tanh-function in expressions (5.13) and (5.14), respectively, assume the value 1;

$$\delta_n = \mu^{-n/(N+1)}(b_n b_{n+1})^{-\frac{1}{2}} = \frac{2}{\pi}\left(\frac{64\mu}{9\pi^4 N}\right)^{-n/(N+1)} \quad \text{for} \quad n = 1, \ldots, N-1,$$

$$\delta_N = \mu^{-N/(N+1)}(2b_N^{-1}\hat{I})^{\frac{1}{2}} = \frac{16}{3\pi^2}\left(\frac{64\mu}{9\pi^4 N}\right)^{-N/(N+1)}.$$

It goes without saying that the solution given just above is by no means established rigorously. It is, however, possible to test this solution numerically. We turn next to this test.

6. Numerical computation of the two-α solution

For the numerical solution of (3.15) it is convenient to replace the normalization condition (5.1) by

$$\langle|\boldsymbol{\theta}|^2\rangle = \mu. \tag{6.1}$$

Using this condition and relation (3.24) we rewrite (3.15) in the form

$$\theta_n'' - \alpha_n^2\theta_n + \frac{1}{2}\frac{\alpha_n \sum_m \langle\theta_m^2\rangle}{\sum_m \alpha_m \langle\theta_m^2\rangle}\left(R + \sum_m [\langle\theta_m^2\rangle - \theta_m^2]\right)\theta_n = 0 \tag{6.2}$$

with

$$\alpha_n = \langle\theta_n'^2\rangle^{\frac{1}{2}}\langle\theta_n^2\rangle^{-\frac{1}{2}}.$$

We expand each function θ_n in terms of a complete system of orthogonal functions which satisfy the boundary conditions at $z = 0, 1$. The simplest system of this kind is provided by the trigonometric functions. Hence we obtain

either

$$\theta_n = \sum_\mu a_{\mu n} \sin(2\mu - 1)\pi z, \tag{6.3a}$$

or

$$\theta_n = \sum_\mu a_{\mu n} \sin 2\mu\pi z, \tag{6.3b}$$

depending on whether θ_n is symmetric or antisymmetric in z. In analogy with linear eigenvalue problems it seems likely that symmetric and antisymmetric forms of θ_n are alternating. However, we have not been able to prove such a property. The numerical investigation shows that the two-α solution consists of a symmetric function θ_1 and an antisymmetric function θ_2. All attempts to generate a two-α solution with symmetric functions θ_1 and θ_2 failed in the region of Rayleigh numbers R which were numerically accessible.

The numerical determination of the two-α solution proceeds by multiplying equations (6.2) with $2\sin(2\nu - 1)\pi z$ and $2\sin 2\nu\pi z$ after the representations (6.3a) and (6.3b) for θ_1 and θ_2, respectively, have been introduced. Averaging of the equations yields a system of algebraic equations for the unknown coefficients $a_{\nu n}$. These equations are solved by a relaxation process. The $(m+1)$th approximation for the unknown $a_{\nu n}$ is obtained from the mth approximation $a_{\nu n}^{(m)}$ by replacing the zero on the right-hand side of the equations by

$$(a_{\nu 1}^{(m+1)} - a_{\nu 1}^{(m)})\,[(2\nu - 1)^2\pi^2 + \alpha_1^2]\,h^{-1},$$

and

$$(a_{\nu 2}^{(m+1)} - a_{\nu 2}^{(m)})\,[(2\nu\pi)^2 + \alpha_2^2]\,h^{-1}$$

for $n = 1$ and 2 respectively. This relaxation process resembles a time-dependent problem in which a non-stationary solution approaches the stationary solution asymptotically, starting from arbitrary initial conditions. The step size h has to be chosen sufficiently small to ensure numerical stability. The number of equations to be integrated has to be finite, of course. The number of coefficients

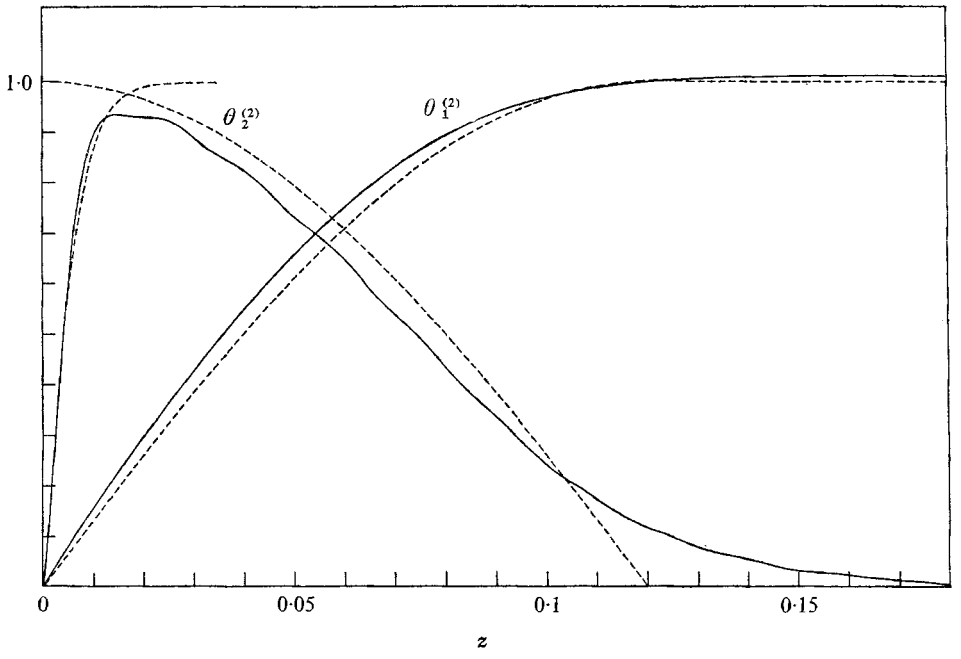

FIGURE 1. The two-α solution. Graph of the functions $\theta_1(z)$ and $\theta_2(z)$ for $R = 50\pi^2$. ——, numerical computation; – – – – boundary-layer theory.

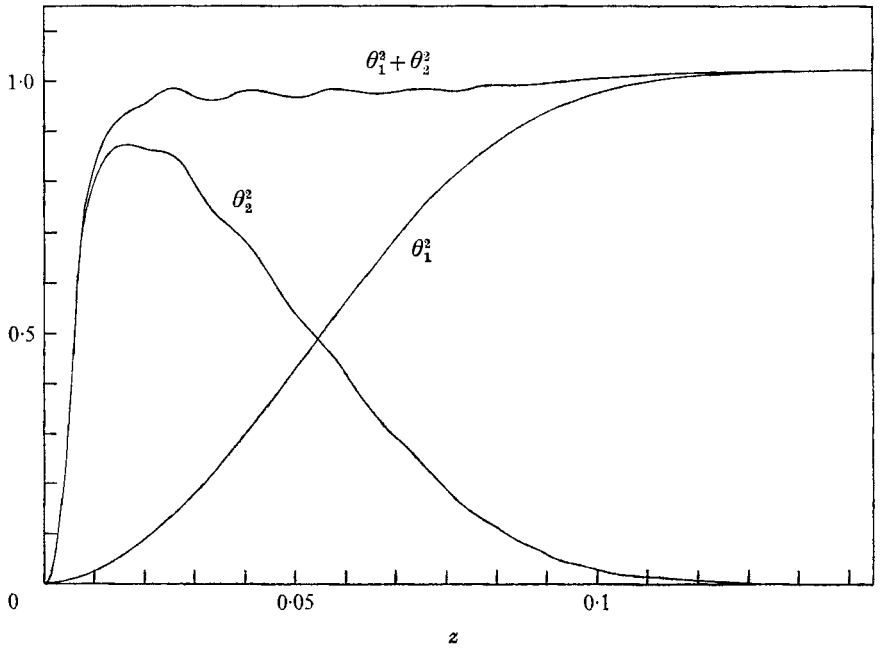

FIGURE 2. The two-α solution as given by numerical computation. The assumption in the boundary layer that $\theta_1^2+\theta_2^2 \approx 1$ in the boundary region where θ_1^2 and θ_2^2 are non-vanishing seems to be valid here even though $R = 50\pi^2$ is not yet asymptotic.

$\alpha_{\nu 1}$ and $\alpha_{\nu 2}$ which have been taken into account is the same. We call this number M. For relatively low values of R good convergence has been obtained for $M = 12$. In the case of higher R the boundary-layer structure poses difficulties. Even for $M = 30$ the Gibbs phenomenon caused by the steep slope at the boundary is still noticeable at $R = 50\pi^2$. Since the step size h has to be decreased as the number $2M$ of equations increases, the limitations of computer time did not allow us to carry the computations much further.

Apart from the oscillations caused by the truncation, the comparison in figure 1 shows that the numerical results and the boundary-layer theory agree reasonably well, even though the Rayleigh number $R = 50\pi^2$ can barely be regarded as representative for asymptotic values. The main difference seems to be that the numerical representation of θ_2 does not show a sudden drop to zero, like that assumed in the boundary-layer analysis. In fact, since it is likely that solutions θ_n of (6.2) are analytic functions of z, it must be assumed that they are non-vanishing throughout the layer except for discrete zeros. The numerical calculations indicate, on the other hand, that θ_2 approaches zero sufficiently fast for the contribution θ_2^2 in the nonlinear term of (6.2) to become negligible at about the same point as that at which $\tilde{\theta}_2$ vanishes. Since only θ_2^2 is of importance as far as the minimum of the functional is concerned, the assumption made in the boundary-layer analysis seems to be well justified. The numerical dependence of θ_1^2 and θ_2^2 and the sum $\theta_1^2 + \theta_2^2$ are shown in figure 2.

The results for the upper bound on the Nusselt number $Nu = 1 + \mu/R$ are shown in figure 3 in comparison with the asymptotic relations in the cases $N = 1$ and 2 derived by the boundary-layer analysis. In contrast to the finite change in slope at the transition from $N = 1$ to $N = 2$ suggested by the asymptotic results, we find that a smooth transition takes place. As the Rayleigh number approaches $R_2 = 113$ from above, the function θ_2 tends gradually to zero. Throughout the range in which the two-α solution exists the value $\mu^{(2)}(R)$ is larger than the value $\mu^{(1)}(R)$. The dependence of the wavenumbers $\alpha_1^{(1)}$, $\alpha_1^{(2)}$ and $\alpha_2^{(2)}$ on R is shown in figure 4. In accordance with the properties of the two-α solution discussed above, the value $\alpha_1^{(2)}$ has to merge with $\alpha_1^{(1)}$ as the Rayleigh number R_2 is approached. Because of the gradual merging of the two-α solution with the single-α solution the numerical scheme described above is not well-suited for the determination of the critical value R_2 of the two-α solution. For the latter purpose a linear perturbation analysis was employed. The equation

$$\theta_2'' - \alpha_2^2 \theta_2 + (\alpha_2/2\alpha_1)\,(R + \langle\theta_1^2\rangle - \theta_1^2)\,\theta_2 = 0 \tag{6.4}$$

was solved by a Runge–Kutta integration method using the boundary conditions $\theta_2 = 0$ at $z = 0, \frac{1}{2}$. In place of the solution θ_1 in terms of elliptic integrals derived in § 4 the approximation

$$\theta_1 \approx 2K \tanh Kz$$

with K given by $R = 8K(4K-6)/(3K-6)$ was used; this differs from the exact solution by less than a fraction of 1 % for Rayleigh numbers in the neighbourhood of R_2. The calculations established that the lowest value of R at which a solution of (6.4) exists is $R_2 = 113{\cdot}07$, corresponding to a wavenumber $\alpha_2 = 11{\cdot}296$. The z dependence of θ_2 is shown in figure 5.

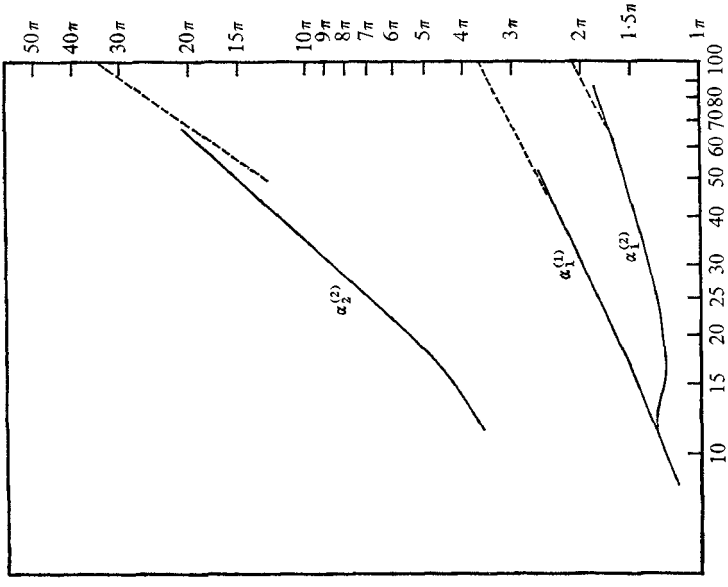

FIGURE 4. The two-α solution. Dependence of the two wavenumbers $\alpha_1^{(2)}$ and $\alpha_2^{(2)}$ on R. Also shown is the dependence of the single-α wavenumber $\alpha_1^{(1)}$ on R. ——, numerical computation; – – – –, boundary-layer theory.

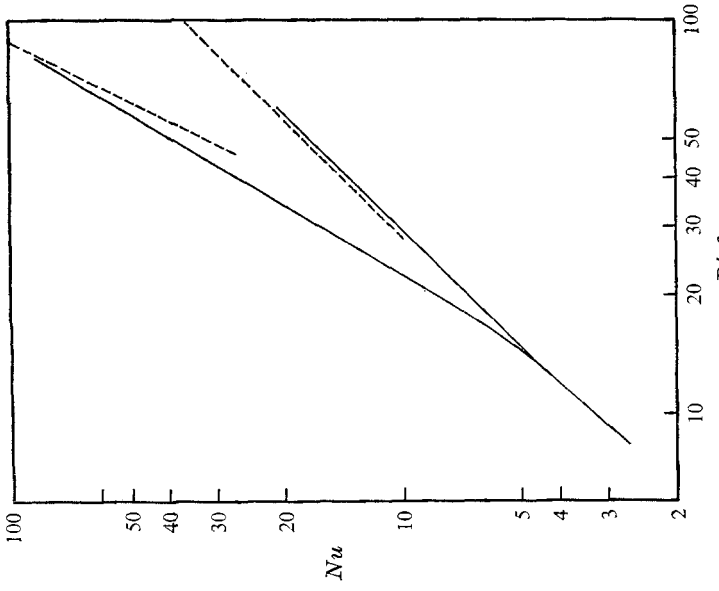

FIGURE 3. The heat transport curve. The top line is the graph of the two-α solution. The bottom line is the graph of single-α solution. ——, numerical computation; – – – –, boundary-layer theory.

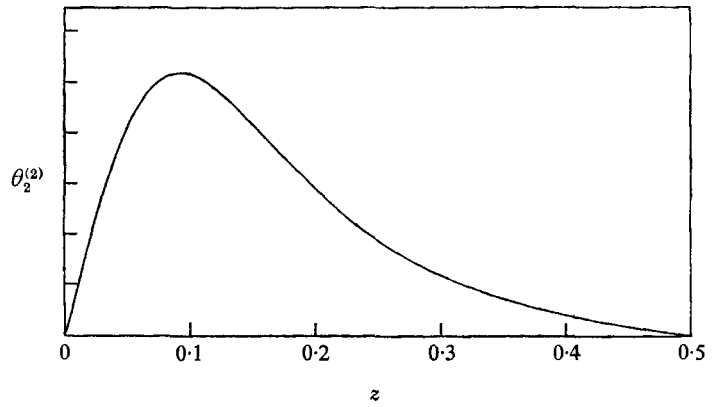

FIGURE 5. The form of $\theta_2^{(2)}(z)$ at $R = 113$, when the two-α solution first appears as an infinitesimal perturbation of the single-α solution (see equation (6.4)). $\theta_2^{(2)}$ has been normalized by setting $d\theta_2^{(2)}(0)/dz = 1$.

7. Comparison with experiment

In figure 6, we have compared the bounds given by the single-α and the two-α solutions with experimental values (Schneider 1963; Elder 1967; Katto & Masuoka 1967; Combarnous & LeFur 1969). A very wide range of porous materials is represented in these experiments. These experiments are in good agreement with the theoretical stability results which give instability (Lapwood 1948) when $R > 4\pi^2$ and global stability (Westbrook 1969) when $R < 4\pi^2$.†

The very good agreement between the observations and the theoretical single-α bound F_1 which is evident when $R < 113$ is supported theoretically by the result summarized by (4.16). The excellent agreement between experiments and the single-α solution for $10^4 > R > 113$ is not explained by the present theory since at $R = 113$ the single-α solution bifurcates and the two-α solution is then the relevant theoretical result. At yet higher values of R we would expect the relevant result to be an N-α solution with successively higher values of N.

Though the quantitative agreement between the observations and the two-α solution is not good the experiments of Combarnous & LeFur are in qualitative agreement with the present theory in the following sense: both theory and experiment indicate that at a sufficiently high Rayleigh number a bifurcation of the convective motion into a new motion of more complicated form occurs. In the theory the more complicated motion is the two-α solution, which comes in at $R \approx 113$ and $Nu \approx 3{\cdot}8$. In the experiments this new motion manifests itself in a

† All but the first mentioned in the list of experiments report errors of about 10% in the determination of the instability point and the heat transport curve. These are attributed by Elder to difficulties associated with determining the thermal conductivity of the saturated medium. It is necessary in porous materials to take the thermal diffusivity as $\kappa = k_m/(\rho C_p)_f$, where k_m is the conductivity of the fluid filled porous solid and $(\rho C_p)_f$ the density times specific heat for the fluid. Katto & Masuoka show that this definition of diffusivity allows one to bring their data, and that of earlier experiments, into agreement with theory. The non-uniformity of the conduction gradient in intrinsically non-uniform porous media is also cited as explanation of the observed small deviations from theory.

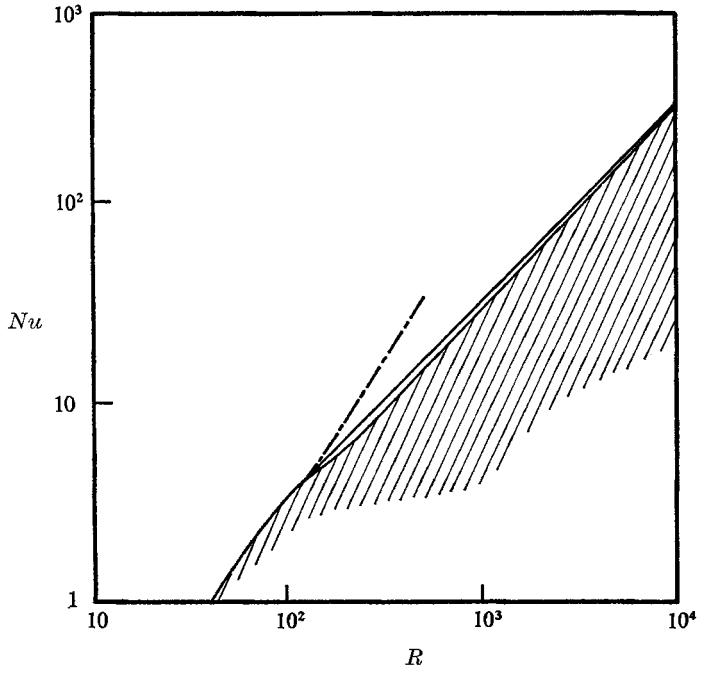

FIGURE 6. Comparison of the single-α Nusselt–Rayleigh number curve (solid line) with experiments (shaded area). — - —, two-α solution.

change in the slope of the heat transport curve at $R \approx 280$, $Nu \approx 6$, a phenomenon which is well known in regular convection and which seems also to occur here in the porous case (see Combarnous & LeFur, figures 2 and 3).

In comparing the bounding theory with experiment it is as well to keep in mind three points. (i) For high Rayleigh numbers ($> 10^6$) the experimental data correlate better with fluid parameters alone. In this regime, according to the rough estimates of Elder, the "boundary-layer thickness is somewhat smaller than the scale of the porous medium". One would not expect the Darcy–Boussinesq equations to hold in these circumstances. (ii) At Reynolds numbers in excess of $O(1)$ based on a pore diameter the form of the Darcy resistance has a more complicated structure than the linear law which leads to (2.1) (see Irmay 1958). (iii) Scaling of the Darcy–Boussinesq equations indicates that the parameter B is very small in most materials. The results of the present analysis apply uniformly to all values of B. An analysis in which $B = 0$ at the start is presently in progress.

This work was partially supported under NSF Grant GA-19605 (FHB) and NSF Grant GK-12500 (DDJ). The major part of the numerical calculations, was carried out on the computer G3 of the Max-Planck-Institut für Physik and Astrophysik, Munich with the help of Mrs Trostel. The interest and assistance of Prof. A. Berman and V. Gupta (Project Themis grant no. 108) with aspects of the work is gratefully acknowledged.

REFERENCES

BUSSE, F. H. 1969*a* *Z. angew. Math. Phys.* **20**, 1–14.

BUSSE, F. H. 1969*b* On Howard's upper bound for heat transport in turbulent convection. *J. Fluid Mech.* **37**, 457–477.

COMBARNOUS, M. & LEFUR, B. 1969 Transfert de chaleur par convection naturelle dans une couche poreuse horizontale. *Comptes Rendus*, **269**, 1009–102.

ELDER, J. W. 1967 Steady free convection in a porous medium heated from below. *J. Fluid Mech.* **27**, 29–48.

HANCOCK, H. 1958 *Elliptic Integrals*. Dover.

HOWARD, L. N. 1963 Heat transport in turbulent convection. *J. Fluid Mech.* **17**, 405–432.

IRMAY, S. 1958 On the theoretical derivation of Darcy and Forcheimer formulae. *Trans. Am. Geophys. Union*, **39**, 702–707.

KATTO, Y. & MASUOKA, T. 1967 Criterion for the onset of convective flow in a fluid in a porous medium. *Int. J. Heat Mass Transfer*, **10**, 297–309.

LAPWOOD, E. R. 1948 Convection of a fluid in a porous medium. *Proc. Camb. Phil. Soc.* **44**, 508–21.

SCHNEIDER, K. J. 1963 Investigation of the influence of free thermal convection on heat transfer through granular material. *11th Int. Cong. of Refrigeration (Munich)*, paper 11–4.

WESTBROOK, D. R. 1969 The stability of convective flow in a porous medium. *Phys. Fluids*, **12**, 1547.